

## DIFFUSIVE TRANSPORT OF MACROMOLECULES ACROSS THE ARTERIAL WALL

Jae Young Kim and Byung Jun Yoon<sup>†</sup>

Department of Chemical Engineering, Pohang University of Science and Technology, Pohang 790-784, Korea  
(Received 21 February 1997 • accepted 16 May 1997)

**Abstract** – A mathematical model of diffusive transport of macromolecules across the arterial wall was developed in order to analyze the enhancement of molecular transport into the media in the presence of the endothelial injuries. The model is based on the continuum description of the distribution of macromolecules in the arterial wall with multiple injuries periodically dispersed on the endothelial surface. A boundary element method is successfully employed to model the problem geometry along with the relevant boundary conditions. The concentration and surface flux are computed for various physical conditions of the artery. Among other factors, the proper estimation of the mass transfer resistance, characterized by the Biot number, of the endothelial surface is crucial for the analysis. In addition the curvature effects are negligible when the vessel radius is larger than 10 times the wall thickness.

**Key words** : Boundary Element Method, Endothelial Transport, Endothelial Injury, Arterial Wall, Atherogenesis

### INTRODUCTION

Abnormal transport of macromolecules such as LDL, albumin, and fibrinogen from the blood stream across the artery wall is an important factor in the early development of arterial disease [Getz, 1990; Weinbaum and Chien, 1993; Ylä-Herttuala, 1991]. The inner surface of the normal arterial wall is completely covered with the endothelial cells which effectively control the transport of macromolecules. When endothelial cells are injured or disturbed by either hemodynamic or biochemical factors, the transport characteristics of macromolecules are substantially altered [Ross, 1986]. The alteration is usually accompanied with the enhanced endothelial permeability to macromolecules. It is generally believed that the intima region of high permeability of macromolecules is prone to the formation of lesion in atherosclerosis [Nerem, 1992].

The transport of macromolecules across the normal artery endothelium attributed to two mechanisms: the transendothelial Brownian diffusion of plasmalemmal vesicles which contain macromolecules inside, and the filtration and diffusion of macromolecules through the intercellular cleft between the adjacent endothelial cells. When the endothelial cell is injured, the diffusive flux of macromolecules is significantly increased through the injured area. The endothelial injury generally means not only the morphological changes of the endothelial cell but also the physiological and metabolic impairments of the endothelial cell. In addition to actual endothelial injury, the normal process of cell turnover leads to a transition state in which the junctional complexes between cells becomes more diffuse, which results in the increased transendothelial transport.

Macromolecules which pass through the endothelium diffuse into the arterial media. The arterial media consists of two parts: the dispersed cellular phase and the continuous interstitial fluid phase. It is believed that macromolecules first diffuse into the in-

terstitial fluid phase, and some of them are eventually transported into the cellular phase. Assuming the concentration of macromolecules is sufficiently high, a continuum description for the distribution of macromolecules in the media can be made. A simple continuum model was first developed by Weinbaum and Caro [1976]. The transport rate is modeled to be proportional to the difference in concentration between the two phases. At steady state the concentrations in both phases are equal, and the concentration distribution satisfies the Laplace equation. In their subsequent analyses [Nir and Pfeffer, 1979; Pfeffer et al., 1981] the artery wall was modeled as a planar slab of uniform thickness and of infinite extent neglecting curvature effects. However, as shown in Table 1 [Fung, 1984], the typical values of the ratio of the inner radius to the wall thickness for human arteries lie between 5 and 10, for which the curvature effects may not be small.

In this work we extend the earlier continuum model [Pfeffer et al., 1981] by analyzing the transport through the cylindrical wall of artery with multiple endothelial injuries. The solution procedure for the cylindrical geometry is facilitated by employing the boundary element method which is especially suitable for the problem of complex geometry with mixed boundary conditions [Beskos, 1987]. The concentration and surface flux of macromolecules are determined for various conditions, and the results

Table 1. Typical size of human arteries

Vessel	Inner radius (mm)	Wall thickness (mm)	Dimensionless radius, R
Ascending aorta	7.5	0.65	11.5
Descending aorta	6.5	0.65	10.0
Abdominal aorta	4.5	0.5	9.0
Femoral artery	2.0	0.4	5.0
Carotid artery	2.5	0.3	8.3
Main pulmonary artery	8.5	0.2	42.5
Arteriole	0.025	0.02	1.2

<sup>†</sup>To whom correspondence should be addressed.

are discussed in order to elucidate the enhancement of the endothelial transport caused by the endothelial injuries.

**MATHEMATICAL MODEL**

According to Weinbaum and Caro [1976], the concentrations of macromolecules in the interstitial fluid phase and the dispersed cellular phase of the arterial wall are represented by

$$\nabla^2 c_1 + \gamma(c_2 - c_1) = \alpha_1 \frac{\partial c_1}{\partial t},$$

$$\gamma(c_1 - c_2) = \alpha_2 \frac{\partial c_2}{\partial t}.$$

Here the subscript 1 and 2 denote interstitial fluid phase and dispersed cellular phase, respectively. The symbol  $c$  is the dimensionless concentration of macromolecules and  $\alpha$  is the volume fraction of each phase. The term  $\gamma(c_2 - c_1)$  accounts for the transport of macromolecules into cellular phase. At steady state, concentration of macromolecules in the interstitial fluid phase is governed by the Laplace equation:

$$\nabla^2 c = 0. \tag{1}$$

Here we drop the subscript 1 for simplicity. In this study the concentration is normalized such that the dimensionless concentration at lumen is 1 and the dimensionless concentration at adventitia is 0. A portion of the arterial wall considered in our analysis is schematically shown in Fig. 1. The injuries of rectangular shape are periodically dispersed on the endothelium. Utilizing the periodic nature of the problem geometry, we consider a single repeated unit for the analysis. The geometric scales of the problem domain are normalized to the thickness of the arterial wall so that the wall thickness is set to 1 regardless of the radius of the artery. Since the thickness of the endothelial layer is vanishingly small compared to that of the arterial media, we approximate the endothelial layer as a surface at  $r=R$ . The size of single injury is represented by the half distances  $\epsilon$  and  $\delta$  along the axial and radial directions, respectively. The linear dimension of single endothelial cell is about 20  $\mu\text{m}$ , thus for an artery of the wall thickness of 0.5 mm the value of  $\epsilon$  and  $\delta$  is around 0.02. The half distances between the injuries along the axial and radial directions are denoted by  $\zeta$  and  $\eta$ , respectively.

We solve Eq. (1) for the repeated unit of the arterial wall shown in Fig. 1 with the following boundary conditions:

$$\frac{\partial c}{\partial r} = -\sigma(1-c) \quad \text{for } S_e^n, \tag{2}$$

$$c = 1 \quad \text{for } S_e^i, \tag{3}$$

$$c = 0 \quad \text{for } S_a, \tag{4}$$

$$\frac{\partial c}{\partial n} = 0 \quad \text{for } S_\theta + S_z. \tag{5}$$

The endothelial surface  $S_e$  consists of two parts: the normal surface  $S_e^n$  and the injured surface  $S_e^i$ . At the normal surface the mass flux is proportional to the difference of concentrations at the lumen and the surface [Eq. (2)]. The proportionality constant  $\sigma$  is known as the Biot number which depends on the hemodynamic conditions in lumen, the surface properties of the endothelium, and other factors [Lever and Jay, 1990]. When  $\sigma=0$  the

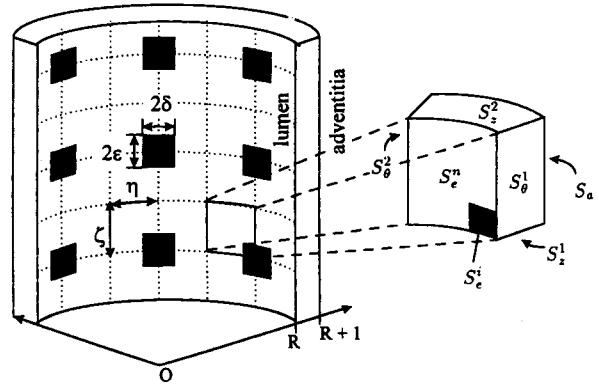


**Fig. 1. Schematics of a portion of artery with a periodic injuries on the endothelium.**

endothelial surface becomes impermeable, and as  $\sigma$  increases the mass transfer resistance across the endothelial surface decreases. Thus, the role of the endothelium as a principal barrier for the mass transport completely disappears when  $\sigma=\infty$ . The appropriate value of  $\sigma$  for normal endothelium must be determined from experimental observations. At the injured surface we assume that the surface concentration is equal to the concentration at lumen [Eq. (3)], which is equivalent to the case of normal endothelium with  $\sigma=\infty$ . With the boundary condition [Eq. (4)] we set the concentration at adventitia as a constant value. The last boundary condition [Eq. (5)] is the symmetric condition, where  $\partial/\partial n$  is the normal derivative in the outward direction to each surface.

The analytical approach for solving Eq. (1) with the relevant boundary conditions is very complicated and not practical. The boundary element method can be conveniently applied to this type of problem. Applying Green's second identity, the Laplace equation transforms into an integral equation [Jawson and Symm, 1977; Kellogg, 1953]

$$\beta c(\mathbf{x}) = \int_S G(|\mathbf{x}-\mathbf{x}'|) \frac{\partial c(\mathbf{x}')}{\partial n} dS(\mathbf{x}') - \int_S c(\mathbf{x}') \frac{\partial}{\partial n} G(|\mathbf{x}-\mathbf{x}'|) dS(\mathbf{x}'). \tag{6}$$

Here  $G(|\mathbf{x}-\mathbf{x}'|) = 1/4\pi|\mathbf{x}-\mathbf{x}'|$  is the fundamental solution for the Laplace equation. The constant  $\beta$  in the LHS of Eq. (6) has one of the following values:

$$\beta = \begin{cases} 0 & \text{for } \mathbf{x} \text{ outside,} \\ 1/2 & \text{for } \mathbf{x} \text{ on smooth boundary,} \\ 1 & \text{for } \mathbf{x} \text{ inside.} \end{cases}$$

By applying the boundary conditions, Eq. (6) can be rewritten as

$$\begin{aligned} \beta c(\mathbf{x}) = & - \int_{S_\theta} c \frac{\partial G}{\partial n} dS - \int_{S_z} c \frac{\partial G}{\partial n} dS + \int_{S_a} G \frac{\partial c}{\partial n} dS \\ & + \int_{S_e^n} \sigma G dS - \int_{S_e^i} c \left( \sigma G + \frac{\partial G}{\partial n} \right) dS \\ & + \int_{S_e^i} G \frac{\partial c}{\partial n} dS - \int_{S_e^i} \frac{\partial G}{\partial n} dS. \end{aligned} \tag{7}$$

For arbitrary points on the boundary surface Eq. (7) can be solved with  $\beta=1/2$ . This boundary integral equation contains two kinds of unknowns: the concentration  $c$  on  $S_\theta + S_z + S_e^n$  and the normal

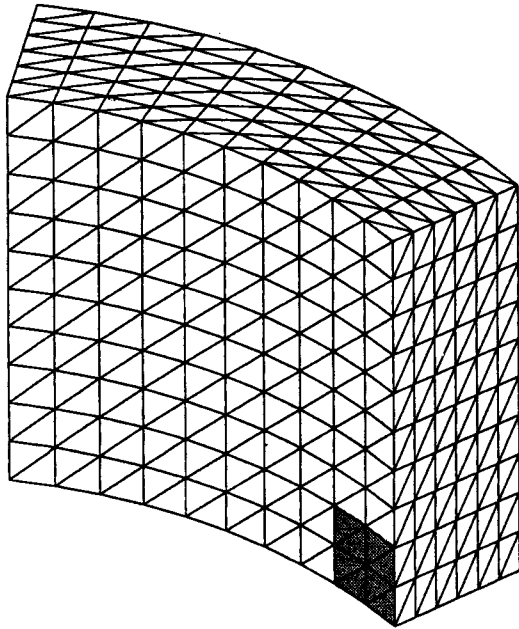


Fig. 2. Discretized surface of the problem boundary.

derivative of the concentration  $\partial c/\partial n$  on  $S_1+S_2^i$ . After solving the boundary integral equation one can readily compute the concentration at any arbitrary points using Eq. (6). The boundary integral equation is solved numerically after discretizing the whole surface of the repeated unit into a number of small boundary elements. In our analysis flat triangular elements are used. Fig. 2 shows the triangulated surface of the repeated unit where the injured region is depicted by a shady area. Depending on the size of the injury we adjust the size of each triangle. We assumed that the unknowns  $c$  and  $\partial c/\partial n$  vary linearly within each triangular element. The problem then reduces to solving for the unknowns at the vertices of each element. The surface integral for each element is performed using Gaussian quadratures [Cowper, 1973].

**NORMAL AND DENUED ENDOTHELIUM**

Before we investigate the transport across periodically injured endothelium, we first consider the transport through normal endothelium as well as through completely denuded endothelium. These limiting analyses are important, since they furnish the limiting behaviors valuable to check the results of the full analysis, and also by comparing the two limiting cases one can determine the Biot number  $\sigma$ . Eq. (1) can be readily integrated for both cases to obtain

$$c^d(r) = \frac{\ln\left(\frac{r}{1+R}\right)}{\ln\left(\frac{R}{1+R}\right)}, \tag{8}$$

$$c^n(r) = \frac{\ln\left(\frac{r}{1+R}\right)}{\ln\left(\frac{R}{1+R}\right) - \frac{1}{\sigma R}}, \tag{9}$$

where  $c^d$  and  $c^n$  correspond to the concentration distributions in the media with denuded and normal endotheliums, respectively. The dimensionless mass fluxes at the endothelial surface for both cases are given by

$$\Psi^d = -\frac{1}{R \ln\left(\frac{R}{1+R}\right)}, \tag{10}$$

$$\Psi^n = \frac{1}{\frac{1}{\sigma} - R \ln\left(\frac{R}{1+R}\right)}. \tag{11}$$

Note that Eqs. (9) and (11) approach Eqs. (8) and (10), respectively, as  $\sigma$  increases.

We plot the dimensionless surface flux as a function of vessel radius in Fig. 3. For normal endothelium three different values of  $\sigma$  are considered: 0.1, 1.0, and 10. As  $\sigma$  increases, the resistance to the transendothelial transport decreases, thus the

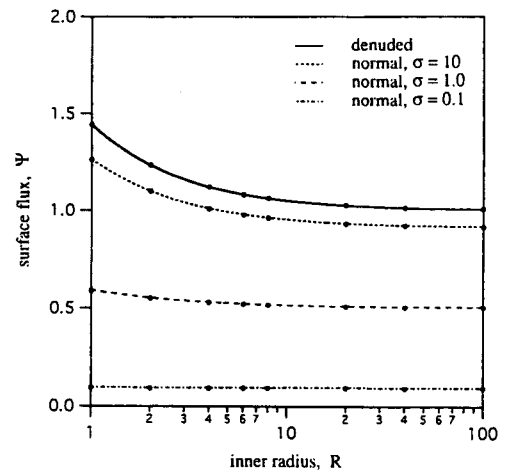


Fig. 3. Dimensionless surface flux as a function of vessel radius for normal and completely denuded endotheliums. Dots are numerical results obtained by the boundary element method.

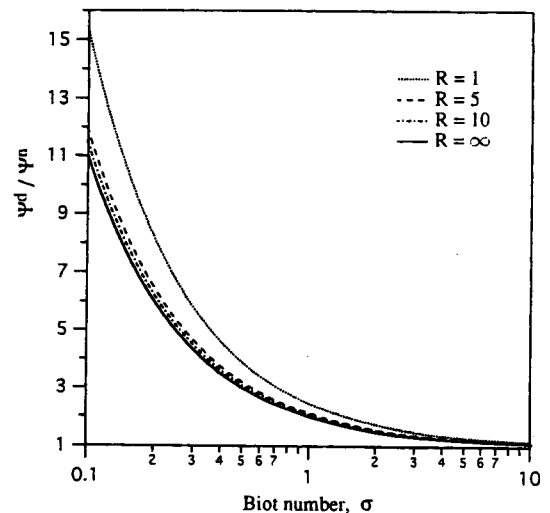


Fig. 4. The ratio of transendothelial fluxes for denuded and normal endotheliums.

flux curve approaches that of denuded endothelium. It has been observed experimentally that denuded endothelium showed enhanced transmural transport [Tedgui and Lever, 1987]. Fig. 3 suggests that when  $\sigma=1.0$ , the denuded endothelium may result in about two times increase of the transendothelial transport. In order to estimate the enhancement rate of the endothelial transport the ratio  $\Psi^d/\Psi^n$  is plotted in Fig. 4 as a function of  $\sigma$ . As  $\sigma$  increases the enhancement becomes marginal. Fig. 4 can be useful for estimating the value of  $\sigma$  of normal endothelium by experimentally determining  $\Psi^d/\Psi^n$ .

The curvature effects are also manifested in Figs. 3 and 4. When  $R$  is larger than 10 the values of the surface flux almost approach those for infinite slab, i.e.,  $R=\infty$ . Fig. 4 shows that the enhancement of the transendothelial transport is nearly unaffected by  $R$  when  $R$  is larger than 10. Thus, unless  $R$  is much less than 5, the estimation of  $\sigma$  of the normal artery using Fig. 4 can be performed with the endothelium of planar geometry.

RESULTS

We first test the boundary element method by computing the surface fluxes for normal and denuded endotheliums. The numerical results for selected values of  $R$  are presented as dots in Fig. 3. The agreement is excellent so that the boundary element method is very reliable to produce accurate results for our problem. In Fig. 5 the endothelial surface concentrations are plotted for the case of periodic injuries dispersed on the endothelium. The injury corresponds to the region where the surface concentration is 1. Two different shapes of injuries are considered: square ( $\epsilon=0.1$  and  $\delta=0.1$ ) and rectangle ( $\epsilon=0.2$  and  $\delta=0.05$ ). Note that the half length of the single injury  $\epsilon=0.1$  corresponds to ac-

tual length of 0.05 mm for the artery of thickness of 0.5 mm. For both cases the single injury has the same area and the total surface area fraction  $\phi$  of the injuries ( $\phi=0.01$ ,  $\eta=\zeta=1.0$ ). The dimensionless inner radius of the artery is 5. Two different values of  $\sigma$  are considered:  $\sigma=0.1$  for (a) and (c); and  $\sigma=1.0$  for (b) and (d). Except the region near the injury the surface concentration rapidly approaches the constant concentration. For normal endothelium the surface concentrations for  $\sigma=0.1$  and  $\sigma=1.0$  are 0.0835 and 0.476, respectively. Because of the interactions between the neighbouring injuries, the constant surface concentration far away from the injury in Fig. 5 is larger than the value for the normal endothelium. Since the surface flux is proportional to  $1-c$ , the transport across the endothelial region far away from the injury is reduced comparing with the normal endothelium. The reduction of the transport in this region can be observed from the slope of the concentration profile near the endothelium in Fig. 6.

The concentration distribution within the media is shown in Fig. 6. The system parameters are identical to those used in Figs. 5(a) and 5(b). Since  $R=5$ , the radial coordinate in Fig. 6 ranges from 5 to 6. The cross section of the media considered in Fig. 6 is the surface  $S_\theta^1$  in Fig. 1, i.e., the surface of constant  $\theta$ , which cuts through the center of the injury. Except the region near the

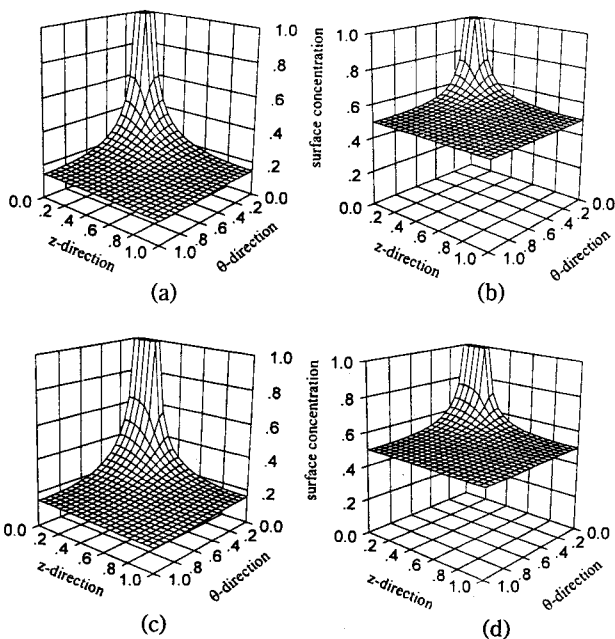


Fig. 5. Endothelial surface concentration with periodic injuries. The inner radius  $R$  is 5, and the total surface fraction of the injury is 0.01. The values of the injury size and  $\sigma$  are (a)  $\epsilon=0.1$ ,  $\delta=0.1$ ,  $\sigma=0.1$ ; (b)  $\epsilon=0.1$ ,  $\delta=0.1$ ,  $\sigma=1.0$ ; (c)  $\epsilon=0.2$ ,  $\delta=0.05$ ,  $\sigma=0.1$ ; (d)  $\epsilon=0.2$ ,  $\delta=0.05$ ,  $\sigma=1.0$ .

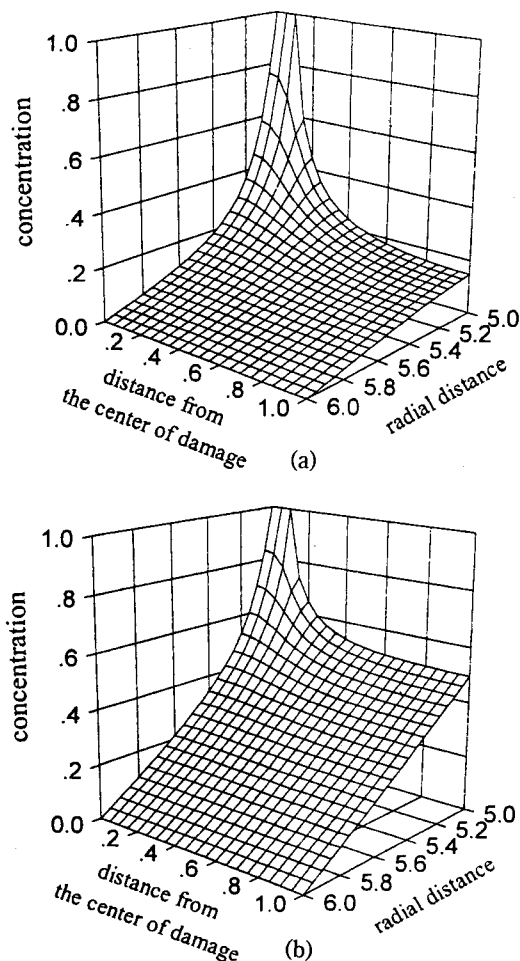
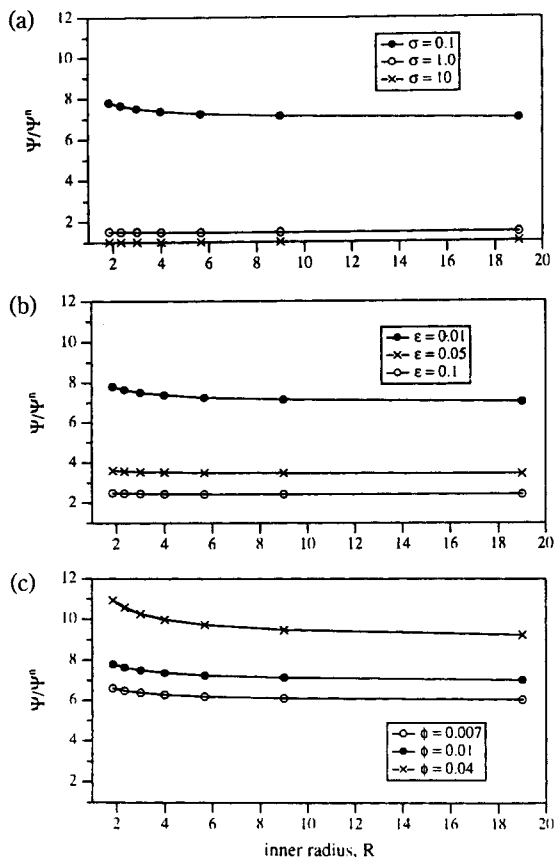


Fig. 6. Concentration distribution of the arterial media with periodic injuries. The inner radius  $R$  is 5, the total surface fraction of the injury is 0.01, the size of the injury is  $\epsilon=0.1$  and  $\delta=0.1$ . The values of  $\sigma$  are (a)  $\sigma=0.1$ ; (b)  $\sigma=1.0$ .



**Fig. 7.** The ratio of transendothelial flux for periodically injured and normal endotheliums as a function of vessel radius  $R$  for various values of  $\sigma$ ,  $\epsilon$ , and  $\phi$ . The reference conditions are  $\sigma=0.1$ ,  $\epsilon=0.01$ , and  $\phi=0.01$ .

injury the concentration approaches almost linearly the value at the adventitia. Compared to the logarithmic variation of the concentration at the normal endothelium [Eq. (9)], the concentration varies more slowly in this region.

The enhancement of the transport across the arterial wall with periodic injuries are summarized in Fig. 7. The effects of Biot number  $\sigma$ , injury size  $\epsilon$ , and the total area fraction of injury  $\phi$  are investigated. The curvature effects are also shown in the Figure. For the reference system we use  $\sigma=0.1$ ,  $\epsilon=0.01$ , and  $\phi=0.01$ . The effects of  $\sigma$  is shown in Fig. 7(a). As  $\sigma$  of normal endothelium increases, the mass transport resistance of normal endothelium decreases, thus the transports across normal and injured endotheliums become indistinguishable. When  $\sigma=10$ , there appears no enhancement of the endothelial transport. The effect of the size of single injury is shown in Fig. 7(b). All 3 curves are for  $\phi=0.01$ , i.e., the population density of the injuries decreases as  $\epsilon$  increases. The case of large number of small injuries results in the bigger enhancement of the endothelial transport than the case of small number of large injuries. This increment is due to the increase of the total area of perimetric region of the injury where the concentration gradient is very steep. When the size of each injury is fixed, the effect of its population density is shown in Fig. 7(c). As the population density (or the total surface fraction of the injuries  $\phi$ ) increases, the enhancement increases. As for the curvature effects, the inner radius  $R$  must be less than 10

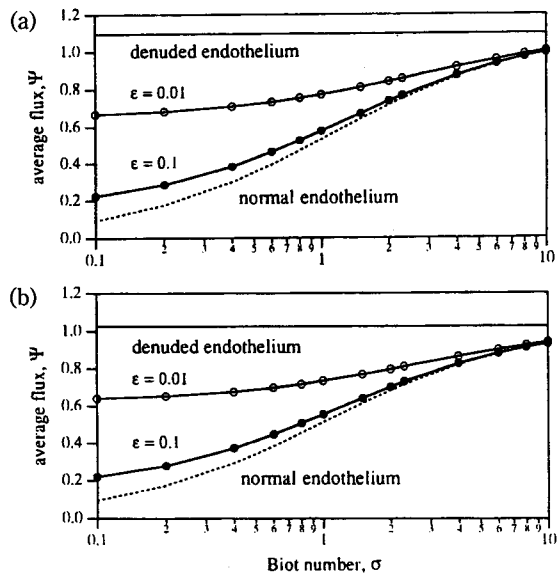


**Fig. 8.** Average transendothelial flux through periodically injured endothelium as a function of  $\sigma$ . The total surface fraction of the injury is 0.01, the values of inner radius are (a)  $R=5$ ; (b)  $R=20$ .

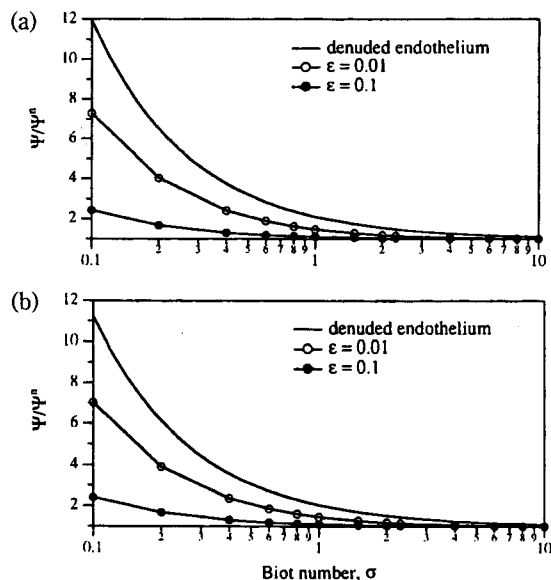


**Fig. 9.** The ratio of transendothelial fluxes for periodically injured and normal endotheliums as a function of  $\sigma$ . The total surface fraction of the injury is 0.01, the values of inner radius are (a)  $R=5$ ; (b)  $R=20$ .

to see any noticeable differences from the case of planar endothelium.

As discussed earlier, a proper choice for the value of  $\sigma$  is crucial for our mathematical analysis to be physically meaningful. In Figs. 8 and 9 the surface fluxes for 3 cases (normal, completely denuded, and periodically injured endotheliums) are plotted and compared as functions of  $\sigma$ . Here the total surface fraction of the injury  $\phi$  is 0.01. Two different values of  $R$  are considered: (a)  $R=5$  and (b)  $R=20$ . As shown in Fig. 7, the case of  $R=20$  can be considered as the case of planar endothelium ( $R=$

$\infty$ ). In Figs. 8 and 9, when  $\epsilon=0.1$ , the curves for  $R=5$  are very close to those for  $R=20$ , thus the curvature effects are negligible. When  $\epsilon=0.01$  and  $\sigma=0.1$ , one can see only 3.8% change of the enhancement rate for the case of  $R=5$  compared with the case of  $R=20$ . Thus, the curvature effect is not significant in this respect.

## DISCUSSION AND CONCLUSION

The major difference between our present model and the previous model [Pfeffer et al., 1981] is the problem geometry. The previous model is based on the planar slab of infinite extent, whereas our model is based on the circular cylinder. Figs. 3 and 7 suggest that the curvature effects are negligible when the inner radius of the artery is larger than 10 times the wall thickness. Aorta and large arteries fall under this category. However, for human arteries of medium and small sizes the curvature effects can be significant.

The endothelial injury results in the enhancement of the transendothelial transport of macromolecules across the injured region, which will eventually lead to the formation of lesion in atherogenesis. When the total area of multiple injuries is fixed, the transendothelial flux increases as the size of single injury decreases. This increase is due to an increase of the endothelial region where the concentration gradient is very steep. The enhancement of the transendothelial transport due to injury is strongly affected by the Biot number  $\sigma$  which characterizes the mass transfer resistance of the normal endothelium. Thus, the proper estimation of  $\sigma$  is very important in our mathematical analysis. By measuring the enhancement rate of the transendothelial flux across the denuded endothelium one may estimate  $\sigma$ . Fig. 4 can be useful for this purpose. As an alternate (or complementary) approach, one may estimate  $\sigma$  theoretically by analyzing the details of the molecular or vesicular transport process across endothelial cells [Tolmin, 1969; Weinbaum and Caro, 1976].

## ACKNOWLEDGMENT

This work was supported by the Korea Science and Engineering Foundation through the Advanced Fluids Engineering Research Center at the Pohang University of Science and Technology.

## NOMENCLATURE

c	: dimensionless concentration
G	: Green function of the Laplace equation
R	: dimensionless inner radius normalized by wall thickness
S	: bounding surface of a repeated unit
$\alpha$	: volume fraction
$\beta$	: constant
$\delta$	: half size of injury along radial direction
$\epsilon$	: half size of injury along axial direction
$\zeta$	: half distance between injuries along axial direction
$\eta$	: half distance between injuries along radial direction
$\sigma$	: Biot number
$\phi$	: total surface fraction of injuries

$\Psi$  : dimensionless mass flux

## Superscripts

d	: denuded
i	: injured
n	: normal

## Subscripts

a	: adventitia
e	: endothelium
1	: interstitial fluid phase
2	: dispersed cellular phase

## REFERENCES

- Beskos, D. E., "Boundary Element Methods in Mechanics", North Holland, Amsterdam, 1987.
- Cowper, G. R., "Gaussian Quadrature Formulas for Triangles", *Int. J. Num. Meth. Eng.*, **114**, 405 (1973).
- Fung, Y. C., "Biodynamics-Circulation", Springer Verlag, New York, 1984.
- Getz, G. S., "The Involvement of Lipoproteins in Atherogenesis", *Ann. N. Y. Acad. Sci.*, **598**, 17 (1990).
- Jawson, M. A. and Symm, G. T., "Integral Equation Methods in Potential Theory and Electrostatics", Academic Press, New York, 1977.
- Kellogg, O. D., "Foundations of Potential Theory", Dover, New York, 1953.
- Lever, M. J. and Jay, M. T., "Transport of Materials through the Walls of Different Blood Vessels", Biomechanical Transport Processes, Mosora, F., Caro, C. G., Krause, E., Schmid-Schönbein, H., Baquey, C. and Pelissier, R., Plenum, New York, 1990.
- Nerem, R. M., "Vascular Fluid Mechanics, the Arterial Wall, and Atherosclerosis", *J. Biomech. Eng.*, **114**, 274 (1992).
- Nir, A. and Pfeffer, R., "Transport of Macromolecules Across Arterial Wall in the Presence of Local Endothelial Injury", *J. Theor. Biol.*, **81**, 685 (1979).
- Pfeffer, R., Ganatos, P., Nir, A. and Weinbaum, A., "Diffusion of Macromolecules Across the Arterial Wall in the Presence of Multiple Endothelial Injuries", *J. Biomech. Eng.*, **103**, 197 (1981).
- Ross, R., "The Pathogenesis of Atherosclerosis-An Update", *N. Engl. J. Med.*, **314**, 488 (1986).
- Tedgui, A. and Lever, M. J., "Effect of Pressure and Intimal Damage on  $^{131}\text{I}$ -albumin and  $^{14}\text{C}$  Sucrose Spaces in Aorta", *Am. J. Physiol.*, **253**, H1530 (1987).
- Tomlin, S. G., "Vesicular Transport Across Endothelial Cells", *Biochim. Biophys. Acta*, **183**, 559 (1969).
- Weinbaum, S. and Caro, C. G., "A Macromolecule Transport Model for the Arterial Wall and Endothelium Based on the Ultrastructural Specialization Observed in Electron Microscopic Studies", *J. Fluid Mech.*, **74**, 611 (1976).
- Weinbaum, S. and Chien, S., "Lipid Transport Aspects of Atherogenesis", *J. Biomech. Eng.*, **115**, 602 (1993).
- Ylä-Herttua, S., "Biochemistry of the Arterial Wall in Developing Atherosclerosis", *Ann. N. Y. Acad. Sci.*, **623**, 40 (1991).